Testing an Aflatoxin B1 Gene Signature in Rat Archival Tissues

ARTICLE *in* CHEMICAL RESEARCH IN TOXICOLOGY · APRIL 2012

Impact Factor: 3.53 · DOI: 10.1021/tx3000945 · Source: PubMed

8 AUTHORS, INCLUDING:

Alex Merrick
National Institute of Environmental Health S…
111 PUBLICATIONS **2,261** CITATIONS
SEE PROFILE

Scott S Auerbach
National Institute of Environmental Health S…
37 PUBLICATIONS **873** CITATIONS
SEE PROFILE

David E Malarkey
National Institute of Environmental Health S…
99 PUBLICATIONS **1,940** CITATIONS
SEE PROFILE

Raymond R Tice
National Institute of Environmental Health S…
19 PUBLICATIONS **1,578** CITATIONS
SEE PROFILE

Published in final edited form as:
Chem Res Toxicol. 2012 May 21; 25(5): 1132–1144. doi:10.1021/tx3000945.

Testing an Aflatoxin B1 Gene Signature in Rat Archival Tissues

B. Alex Merrick[†,*], **Scott S. Auerbach**[†], **Patricia S. Stockton**[†], **Julie F. Foley**[‡], **David E. Malarkey**[‡], **Robert C. Sills**[‡], **Richard D. Irwin**[§], and **Raymond R. Tice**[†]

[†]Biomolecular Screening Branch, Division of the National Toxicology Program, National Institute of Environmental Health Sciences, Research Triangle Park, NC 27709

[‡]Comparative Medicine and Pathology Branch, Division of the National Toxicology Program, National Institute of Environmental Health Sciences, Research Triangle Park, NC 27709

[§]Toxicology Branch of the Division of the National Toxicology Program, National Institute of Environmental Health Sciences, Research Triangle Park, NC 27709

Abstract

Archival tissues from laboratory studies represent a unique opportunity to explore the relationship between genomic changes and agent-induced disease. In this study, we evaluated the applicability of qPCR for detecting genomic changes in formalin-fixed, paraffin-embedded (FFPE) tissues by determining if a subset of 14 genes from a 90-gene signature derived from microarray data and associated with eventual tumor development could be detected in archival liver, kidney, and lung of rats exposed to aflatoxin B1 (AFB1) for 90 days in feed at 1 ppm. These tissues originated from the same rats used in the microarray study. The 14 genes evaluated were Adam8, Cdh13, Ddit4l, Mybl2, Akr7a3, Akr7a2, Fhit, Wwox, Abcb1b, Abcc3, Cxcl1, Gsta5, Grin2c and C8orf46 homolog. The qPCR FFPE liver results were compared to the original liver microarray data and to qPCR results using RNA from fresh frozen liver. Archival liver paraffin blocks yielded 30 to 50 μg of degraded RNA that ranged in size from 0.1 to 4 kB. qPCR results from FFPE and fresh frozen liver samples were positively correlated ($p \leq 0.05$) by regression analysis and showed good agreement in direction and proportion of change with microarray data for 11 of 14 genes. All 14 transcripts could be amplified from FFPE kidney RNA except the glutamate receptor gene Grin2c; however, only Abcb1b was significantly upregulated from control. Abundant constitutive transcripts, S18 and β-actin, could be amplified from lung FFPE samples, but the narrow RNA size range (25–500 bp length) prevented consistent detection of target transcripts. Overall, a discrete gene signature derived from prior transcript profiling and representing cell cycle progression, DNA damage response, and xenosensor and detoxication pathways was successfully applied to archival liver and kidney by qPCR and indicated that gene expression changes in response to subchronic AFB1 exposure occurred predominantly in liver, the primary target for AFB1-induced tumors. We conclude that an evaluation of gene signatures in archival tissues can be an important toxicological tool for evaluating critical molecular events associated with chemical exposures.

Introduction

Formalin-fixed and paraffin-embedded (FFPE) tissues from toxicological studies are a valuable resource for linking histopathological diagnosis to gene expression profiles that can

[*]Corresponding Author: Biomolecular Screening Branch, Division National Toxicology Program, National Institute of Environmental Health Sciences, Research Triangle Park, NC 27709, Ph: 919-541-1531, Fx: 919-541-3715, merrick@niehs.nih.gov.

Notes: The authors declare no competing financial interests.

Supporting Information: Supplemental Table 1. This information is available free of charge via the Internet at http://pubs.acs.org/.

provide insights into the molecular mechanisms of chemical pathologies and disease.[1] Often, only limited numbers of frozen samples of fresh tissues exist for retrospective or hypothesis-driven studies, making archival specimens an especially useful resource. Performing archival expression studies would spare time and resources rather than conducting new in-life studies to create fresh tissue for molecular analysis. For example, the National Toxicology Program (NTP) archives contain more than 5 million paraffin tissue blocks from over two thousand high quality toxicological studies using laboratory animals. Procedures have been developed for the extraction of RNA from FFPE tissues after years in storage.[2, 3] Sample sections cut from tissue blocks or mounted slides can be deparaffinized and enzymatically digested to release nucleic acids for extraction and purification[2].

Genome-wide profiling can be performed upon FFPE samples [4–10], but many probes are insensitive to degraded RNA and the interpretation of gene expression signatures from paraffin tissue must be done carefully since variable RNA quality can reduce the dynamic range of expression signal and miss low copy transcripts.[4, 11, 12] Although less comprehensive than microarray platforms, quantitative PCR (qPCR) is considered one of the most sensitive methods for comparing a wide range of gene expression levels, it is frequently used to confirm signatures generated by microarray platforms and it is reliable even when the RNA is of low amount and quality.[13] qPCR of RNA extracted from clinical FFPE samples is being used to detect the presence of gene signatures in an effort to improve patient diagnosis and to predict therapeutic response.[12, 14, 15] Similarly, our goal was to explore use of qPCR for predictive gene signatures in FFPE tissue blocks stored in a large institutional archive.[16]

In a previous study[17], liver microarray profiling was performed in male F344/N rats exposed subacutely and subchronically to a structurally diverse set of agents, including the liver carcinogen aflatoxin B1 (AFB1).[18–20] The transcript profiles were used to derive predictive computational models for classifying hepatocarcinogens prior to tumor development.[17] Clustering of the most informative probes common to two or more predictive models produced a subset of genes often overexpressed in various malignancies. These included Mybl2[21], the disintegrin metalloprotease Adam8[22], the drug transporter, abcb1b[23] and the DNA-damage sensitive C8orf46 homolog[24], as well as genes that are repressed after genotoxic challenge like Wwox and Fhit that lie within chromosomal fragile sites.[25–27] We selected AFB1 tissue blocks from this study because of significant gene expression response at 90 days exposure and since it is a prototype genotoxic carcinogen. Chronic oral exposure to aflatoxin B1 (AFB1) is known to produce multiple hepatocellular carcinomas in many species, including rat[28, 29], produced by cytochrome P450-mediated formation of the 8,9-epoxide metabolite and induction of DNA adducts that lead to genetic damage and cellular transformation.[19, 30] Although AFB1 causes a majority of treated rats to develop hepatocellular carcinomas within 6–12 months at 1 ppm, a minority develop kidney tumors.[18] Lung is not considered a target organ although occasional pulmonary tumors attributed to metastasis have also been observed.[20] Our hypotheses were that a subset of genes from a previously derived AFB1 gene signature would be observed in archival RNA from fresh frozen liver, would be replicated in FFPE liver and would also be present in other tissues like kidney and lung, as secondary or alternate targets for carcinoma.

Experimental Procedures

Animal treatment and tissue fixation

The tissue samples used in this study were collected in a previously reported study by Auerbach et al.[17] from male F344/N rats exposed to 1 ppm AFB1 in NTP 2000 feed for 90 days, and stored either as fresh frozen or as FFPE in the NTP archives. Feed only animals served as controls. There were six animals per group in control and AFB1 treatments. At

necropsy, rats were anesthetized with carbon dioxide and oxygen to remove blood for serum clinical chemistries prior to sacrifice. After euthanasia, a cross-section of the left and median lobes of the liver were taken and placed into 10% neutral buffered formalin (NBF) for histopathology. The remainder of the left and median lobes was minced quickly into small pieces and flash frozen in liquid nitrogen within 4 min of euthanasia, and stored at −80°C. Similarly, kidneys were cross-sectioned for histopathology. Lungs were carefully removed from the thoracic cavity and inflated with 10% neutral-buffered formalin (NBF), tied off at the trachea and immersed in NBF. Tissues were stored in NBF at room temperature for 24 hr, trimmed, transferred to 70% ethanol for 12–24 hr prior to processing and embedding in paraffin. Sections were prepared at 4–6mm for staining with hematoxylin and eosin for microscopic examination. The same control and AFB1 exposed animals were used for all expression analyses.

RNA extraction and transcript profiling

RNA was obtained from fresh frozen liver as previously described.[17] Briefly, RNA was extracted from 130–150 mg of liver tissue with Qiagen RNeasy Midi kits (Valencia, CA, USA). A 500 ng amount of total RNA was converted into labeled cRNA with nucleotides coupled to fluorescent dye Cy3 using the Low RNA Input Linear Amplification Kit (Agilent Technologies, Palo Alto, CA, USA) according to the manufacturer's protocol. Cy3-labeled cRNA from each sample was hybridized to Agilent Rat Whole Genome Oligonucleotide microarrays in a 4X44K format. Microarray data are available through the NTP Chemical_Effects_in_Biological_Systems (CEBS) database, accessible at http://www.niehs.nih.gov/research/resources/databases/cebs/index.cfm. In this study, RNA integrity for microarrays was evaluated by size distribution of the 18S and 28S ribosomal RNA (Bioanalyzer, Agilent Technologies) in which RIN values for all samples were ≥ 8.8.

RNA Extraction from FFPE Blocks

RNA was extracted from FFPE tissue blocks that had been stored for four years in a thermostatically and humidity controlled archival facility (Experimental Pathology Laboratories Inc., RTP, NC, USA) prior to RNA extraction. From each paraffin block of each animal, three paraffin sections, each 25 micron thick, were obtained under RNase free conditions and combined into a single nuclease free screw cap tube (1.5 mL O-ring, Sardstedt, ThermoFisher Scientific, Waltham, MA, USA) and centrifuged for 15 sec in a microfuge. A commercial kit was used for RNA extraction (Purelink FFPE RNA Isolation Kit, Cat No. K1560–02, Invitrogen); the protocol was modified slightly to accommodate proportional increases in volumes. Briefly, 0.5 mL of a non-volatile (xylene free) melting buffer was added to each tube to completely cover the sections and release tissue from paraffin after 10 min of rotation in an Eppendorf Thermomixer at 72°C. To free nucleic acids from tissue, protein was digested for no more than 1hr at 60°C with Proteinase K (75 μL, 20mg/mL, DNase and RNase free; Worthington, Lakewood, NJ, USA) using thermomixer rotation. Paraffin was then separated from solubilized nucleic acids by centrifugation at 14,000 × g for 1 min. The supernatant was transferred into a nuclease free tube and centrifuged again to separate residual paraffin. In a clean tube, a volume of 600 μL binding buffer was added to 575 μL of solubilized tissue sample, then mixed and divided into two tubes (~580 μL/tube). An aliquot of 600 μL of 100% ethanol was added to each tube and mixed by inversion. Samples of three successive 700 μL aliquots could be loaded onto the same silica-based membrane in a spin cartridge for capture of RNA. Silica spin columns were centrifuged at 800g for 1 min, discarding the flow-through until all lysate was loaded. Impurities were removed with 500 μL of an ethanol-based Wash Buffer, centrifuged at 14,000 × g for 1 min, and repeated twice more for a total of three washes. After the final wash, columns were centrifuged for 2 min to remove any trace of ethanol. RNA was eluted at 14,000g after incubation for 1 min with 30 μL of 65°C RNase-free water. The process

was repeated and aliquots were combined for a 60 μL total sample. Removal of any contaminating DNA was performed for 15 min at room temp in an off-column digestion with 15 μL (7.5 μL 10X buffer, 7.5 μL enzyme) of DNase I (RNase-free, Invitrogen) and the enzyme was inactivated according to protocol. The concentration of RNA (30–50 μg/3 sections) was determined spectrophotometrically (Nanodrop, ThermoFisher, Waltham, MA, USA) and the size range by microcapillary separation (Bioanalyzer, Agilent).

AFB1 signature Genes

Selection of AFB1 signature genes involved a two-fold strategy to sufficiently evaluate use of FFPE samples. First, we chose six top scoring, carcinogen-classifier transcripts from a rat hepatocarcinogenicity study[17] as well as specific genes (eight transcripts) responding to subchronic AFB1 exposure from the same microarray study; second we ensured that fold changes of selected transcripts included down-regulated, moderately changed and up-regulated alterations from control. In the study by Auerbach et al.[17], support vector machine (SVM) learning methods were used to generate hepatocarcinogenicity models from exposure of rats to a collection of hepatocarcinogens that included AFB1, 1-amino-2,4,-dibromoanthraquinone, N-nitrosodimethylamine, and methyleugenol and non-hepatocarcinogens that included acetaminophen, ascorbic acid and tryptophan. A total of 89 probes informed one or more of the optimal SVM models. For the current study, we chose some of the most informative probes[17] to determine their expression in FFPE by qPCR; the ones identified were Wwox, Fhit, Adam8, Mybl2, Abcb1b, and the rat homolog of c8orf46 (RGD1561849). Wwox and Fhit belong to the fragile site gene family and are down-regulated in mouse and rat liver exposed to genotoxic hepatocarcinogens.[25–27] Mybl2 (B-Myb) is a cell cycle regulatory transcription factor found to be elevated in many cancers.[31,32] Adam8 is a member of the disintegrin metalloprotease gene family[33] involved in tissue remodeling, ectodomain shedding of ligands for activation of EGFR[33] and chronic liver diseases and cancer.[33] Abc1b1 (MDR1/P-glycoprotein) is widely known as a drug transporter induced by chemical exposures but may also have a role in tissue repair and regeneration.[34] C8orf46 is a transcript highly upregulated in response to genotoxic carcinogens, including AFB1.[17]

Eight additional genes were selected that were either upregulated at 90 days[17] by the hepatocarcinogens tested, including Akr7a3[35, 36], Abcc3[37], Grinc2c[38], Cdh13[39, 40], Cxcl1[41] and Ddit4l[42, 43], while the latter are known AFB1-responsive genes, Gsta5[36, 44] and Akr7a2[45, 46]. Gene transcripts, corresponding microarray probes, and cellular functions are summarized in Table 1.

qPCR Analysis

Analysis was performed on an ABI Model 7500 Real-Time instrument (Applied Biosystems, Foster City, CA). SuperScript II First Strand cDNA system (Invitrogen) was mixed with RNA from FFPE and fresh frozen samples for reverse transcription using random hexamers. Primers for each gene were designed with Primer3 open source software and checked for a single product amplicon (74–142 bp) by gel electrophoresis. The same primers for each gene were used for fresh frozen and FFPE liver. Microarray probes for each gene can be found in Auerbach et al.[17] cDNA was amplified in a SYBR Green PCR Master Mix (ABI) reaction for 40 cycles in 96 well plates. Use of Sybr Green permitted flexibility in primer design needed in these studies. Each transcript was analyzed by duplicate qPCR reactions from each animal sample. There were six biological replicates (n=6 rats/group) for each transcript in each treatment group (control and AFB1). Gene changes were determined by the $2^{-\Delta\Delta Ct}$ method by normalizing to β-actin expression which did not vary significantly with AFB1 treatment. Primers are summarized in Table 2.

PCR amplification, cloning and sequencing

The aldo-keto reductase, Akr7a3, is highly-induced after AFB1 exposure and represents an important cellular defense against the toxic and mitogenic effects of the dialdehyde metabolite of AFB1.[35, 36] In addition, the size of the Akr7a3 transcript (1272 bp) made it useful for determining amplification size ranges within select Akr7a3 regions using degraded RNA. Akr7a3 amplicons of increasing sizes were prepared by PCR of reverse transcriptase (RT) reactions prepared with random hexamer primers according to the manufacturer's protocol (Invitrogen). PCR amplification reaction mixtures were in a 15 μL volume comprised of 7.5 μL of 2X Hot Start Sweet Master Mix (SABiosciences, Frederick, MD, USA), 0.6 μL primers (100 nM final concentration), 1 μL RT reaction (1 μL cDNA/20 μL reaction) and RNase-free water. Thermocycler conditions for PCR were 95°C for 10 min for polymerase activation, 95°C for 30 sec, 57°C for 30 sec, and 72°C for 30 sec for 35 cycles, followed by 7 min extension at 72°C. PCR products were separated by 2% agarose gel electrophoresis and detected by ethidium bromide fluorescence. The following primer pairs were used to produce amplicons of varying sizes based on the rat Akr7a3 transcript (NM013215). The 5′Utr (For) primer, CTTACCCTCCACCTTCTTCT, was paired with 1st exon (Rev) primer, AGGTCTCCTAGGATGGTCTC for a 211 bp product; with 2nd exon (Rev) primer, TTCAGTGTCTTCCCAAACAT for a 289 bp product; with 2nd exon (Rev) primer, CTCTTCAGTGACGTCTCCAG, for a 331 bp product; with 3rd exon (Rev) primer, CAGAGGGTACAAATCTCAGC, for a 499 bp product; and with the 7th exon (Rev) primer, GTTCCAGGCTTGGTCAAA, for a 988 bp product. The 1st exon (For) primer, AGACCATCCTAGGAGACCTG, was paired with a 2nd exon primer, CGTGGTCTGGAAAGTGTAAA, for a 189 bp product; and with a 2nd exon primer, GACACTGCAGCCTCTTCA, for a 150 bp product. The 2nd exon (For) primer, TAAAAATTGCCACCAAGG was paired with a 2nd (Rev) exon primer, CTATAGGAGTGCCGTGGTCT, for a 150 bp product.

PCR-cloning reactions for the entire coding regions of both Akr7a3 and Ddit4l were also conducted that were similar to the preceding section used to amplify products for cloning and sequencing. In these experiments, oligo-dT was used in reverse transcription of Akr7a3 transcript and oligo-dT or random hexamers were used in reverse transcription of Ddit4l transcript. Primers were designed to amplify two separate amplicons whose sequences overlapped in order to cover the entire coding region of each transcript. For Akr7a3 (NM_013215), primers were synthesized for amplicons of lengths at 538 bp (For, TGGAACCAACGTCCTCTC and Rev, GCATGATCCAGCCATTTT) and 751 bp (For, GAGGGCAAGTTTGTGGAG and Rev, GCTCAGCCAGCTCTCACT). Primers were made for Ddit4l (NM_080399) amplicons for 296 bp (For, TGCACGTGAACTTGGAAA and Rev, AGCCACTCATTAGGGACCTT) and 513 bp (For, CCTTCAGCGTCTGGTGAAAT and Rev, AGCAGCTCTCCTGCTTGAAC) sizes. Briefly, amplicons were gel purified in 2% agarose, cut out, melted and purified on silica gel spin columns (Qiagen, Valencia, CA, USA) and TOPO TA cloned into chemically-competent *Escherichia coli* (TopTen cells, Invitrogen) according to the manufacturer's protocol. Transformed cells were selected for positive clones on 50 μg/mL Kanamycin LB agar dishes and screened for inserts by agarose gel electrophoresis prior to Sanger sequencing of plasmids using forward and reverse M13 sequencing primers (Forward: GTAAAACGACGGCCAG; Reverse: CAGGAAACAGCTATGAC). At least 4 sequences were obtained for each amplicon from two different animals.

RESULTS

qPCR analysis of Fresh Frozen and FFPE liver

A 14 gene signature was selected for evaluation by qPCR of RNA from fresh frozen and FFPE liver tissues. Genes were chosen on the basis of their change in expression in SVM models for hepatocarcinogens or responsiveness to AFB1 based on results in our prior study.[17] qPCR data were normalized by β-actin expression (not altered by AFB1), which were compared to Agilent microarray fold changes. Expression analysis using RNA from samples of fresh frozen and FFPE liver for qPCR and for microarray were from the same control and AFB1 90 day exposed animals. Fold changes were transformed to $\log^2$ scale and are presented in Figure 1.

Gene expression generally agreed in direction and proportion of change for 11 of 14 genes. Such genes included highly upregulated transcripts like cdh13, moderately upregulated transcripts such as Mybl2 and Abcc3, and the downregulated transcript, Fhit. Of these 11 genes, 4 genes (Adam8, C8orf46, Ddit4l and Abcb1b) showed quantitative differences ($p<0.05$) among the three expression conditions. Also, fresh frozen RNA had less expression changes for C8orf46 and Ddit4l compared to FFPE and microarray data. Three genes (Cxcl1, Grin2c, Wwox) showed directional expression changes, which were not uniform and were significantly different among groups for Wwox and Grin2c. Most notable was that the expression of Grinc2c in fresh frozen RNA was down regulated compared to control but upregulated in FFPE and microarray expression formats. Despite this one exception, expression changes using RNA isolated from FFPE tissue were found to be highly reproducible and in agreement with microarray analysis and qPCR data from fresh frozen tissue for 78% of the signature genes surveyed.

Correlation analysis of *fresh frozen* and FFPE liver gene expression

Regression analysis of gene changes from all 14 genes for each animal using fresh frozen and FFPE RNA showed a significant correlation coefficient of 0.73 (Figure 2A). Notably, data tended to be more scattered at low expression levels (<3) compared to higher expression values. Figure 2b shows the data plotted by principal components. Principal component analysis (PCA) is a data reduction tool to better visualize complex, high-dimensional data sets into three-dimensional space that may better reveal group relationships. Here, the PCA plot of expression data accounted for 76.8% of the total variability and revealed animals from each expression platform clustered distinctly from the other two platforms. The plot suggests consistency and reproducibility of qPCR expression data derived from degraded FFPE RNA compared to the other two platforms (fresh frozen and microarray) using intact RNA.

Molecular sizing of liver RNA and qPCR amplification plots

Molecular sizing of fresh frozen and FFPE liver RNA and amplification curves for constitutive and AFB1-responsive genes are shown in Figure 3. Figure 3A shows the comparability of molecular size ranges of control and AFB1 FFPE liver RNA from representative samples. Separation of fresh frozen RNA (inset Figure 3A) shows sharp 18S and 28S peaks that approximate their true, respective 2kb and 5kB molecular sizes that are consistent with intact RNA preparations. The RIN (RNA integrity number) values for RNA from fresh frozen control and AFB1 groups were 8.34 ± 0.11 and 7.80 ± 0.11, respectively. By comparison, FFPE RNA separated as a skewed singular peak ranging from 25–4000 nucleotides (nt) in which much of the RNA population was at ≤1000nt. RIN values for FFPE liver RNA indicated a degraded state of the RNA and ranged from 2- 2.5. The size and shape of molecular sizing profiles for FFPE liver RNA were comparable within the six

samples of each group and between control and AFB1 groups, suggesting the amount of RNA degradation was similar among samples.

Despite RNA degradation in FFPE samples, the amplification plots in Figure 3B in qPCR analyses demonstrated high reproducibility among individual samples for β-actin expression for which Ct values were similar between the two groups. Further, expression of three AFB1-responsive genes (Cdh13, Adam8 and Abcb1b) showed consistent reductions in Ct values compared to control, which upon normalization using β-actin resulted in multiple fold induction of these three genes and several others as shown in Figure 1.

Amplicon size Limits of FFPE RNA

We were also interested in using FFPE RNA for other molecular analyses in addition to qPCR analysis, which favors generation of short amplicons. We wanted to determine how large an amplicon could be produced by standard PCR conditions using degraded RNA isolated from FFPE liver. To address this question, primers were designed to amplify regions of increasing size of the AFB1-responsive gene, Akr7a3. Amplicons were designed from the 5′-Utr region extending to sequences within exons 1, 2, 3 and 7 and also from exon 1–2 and exon 2 alone to create PCR products ranging from 150nt to 988nt in length. cDNA was created from identical inputs (1 μg) of either fresh frozen RNA or FFPE RNA in reverse transcriptase (RT) reactions primed with random hexamers. The same volumes (1 μL) from each RT reaction were then amplified by PCR for 35 cycles and the reaction products were separated on agarose gels. Results of a representative experiment are shown in Figure 4. Amplicons of similar intensity were observed for fresh frozen liver RNA from 150 to 499 bp and a fainter band could be found at 988 bp. In comparison, PCR of FFPE liver RNA produced amplicons of visible but diminishing intensity from 150 to 499 bp and the longest amplicon (988 bp) was not detectable. These experiments demonstrate that FFPE RNA from liver could be used for amplification of transcript sequences of substantial size (up to 500 bp).

PCR Cloning and sequencing of Akr7a3 and Ddit4l

In addition to qPCR, amplification and sequencing of an entire transcript from target tissues can provide more comprehensive data about gene expression including potential nucleotide variations from reference genomes. PCR cloning of the protein coding regions of two AFB1-responsive genes, Akr7a3 and Ddit4l, was performed (Figure 5). Two PCR products of the rat mRNA Akr7a3 (NM_013215; 1272 nt in length, CDS 71–1054 nt) were generated with overlapping sequences from 13 to 551, and 507 to 1209, respectively. PCR products were isolated, cloned and sequenced; the cumulative results showed identical alignment with the known mRNA sequence for rat Akr7a3. Similarly, rat mRNA Ddit4l (NM_080399; 1107 nt in length, CDS 439–1020 nt) was amplified into two overlapping products from 361–874 nt and 761–1059 nt, respectively. Sequencing results were highly similar for the consensus sequence of Ddit4l except for a synonymous T→C substitution that was consistently observed at the third base of codon 40. Fresh frozen RNA was used to establish the baseline sequence for these two genes, although these results can be duplicated with appropriately sized products using FFPE RNA. For example, we found that amplification products from FFPE RNA, such as the 299nt length Ddit4l fragment exhibited the identical sequence as fresh frozen RNA.

Testing AFB1 gene signature in kidney and lung

We wanted to determine if the AFB1 gene signature present in liver was present also in kidney and lung, two other organs for which tumors have been found after chronic AFB1 exposure. Gene expression changes from qPCR of RNA extracted from FFPE kidney are shown in Figure 6. Normalized ΔCt values ($Ct^{transcript} - Ct^{\beta\text{-}Actin}$) allow comparison

between control and AFB1 groups for each transcript. Data showed that all genes were reproducibly expressed in all RNA samples extracted from FFPE kidney except for Grin2c whose expression was not detected. Transcript changes for all genes were similar in direction and magnitude between the two treatments with the exception of slight variations in Akr7a2. However, only Abcb1b expression was significantly increased at 2.8 fold above control in AFB1 exposed rats. qPCR analysis of these genes in lung did not result in usable data since the RNA was characterized by poor amplification and high Ct values despite large inputs of cDNA (1–4 μL) of reverse transcriptase reactions.

Comparative molecular sizing and gene expression in FFPE liver, kidney and lung

The preceding observations led us to evaluate molecular sizing of RNA isolated from these three FFPE tissues to better compare expression data. Electrophoretic separations of representative samples from each tissue are shown in Figure 7A. Molecular sizing of comparable RNA loads of control liver, kidney, and lung during the same electrophoresis analysis suggests the population ranges were 25–4000 nt, 25–2000 nt and 25–500 nt, respectively. RIN values were ≤ 2.5 for all tissues. For liver, the fluorescence intensity curve returned to baseline (0 fluorescence units) at about 4000 nt but in kidney leveled off at 2000 nt while not quite reaching baseline. Notably, the shape of the fluorescence curve for FFPE lung RNA was less complex and narrower than for liver and kidney, returning to baseline at 500 nt. We also observed that for each tissue, RNA separation profiles did not differ between control and AFB1 groups (data not shown). Other investigators have noted that mRNA levels of constitutive genes are generally at similar levels of expression across various tissues using qPCR after comparable cDNA inputs[47] so we tested the expression of two housekeeping genes in liver, kidney and lung to determine if there was a relationship between RNA sizing and gene expression. In Figure 7B, qPCR of constitutive genes, β-actin and S18, enabled an orthogonal measure of RNA integrity among FFPE tissue samples in addition to molecular sizing. Using equal cDNA inputs for qPCR reactions, we found that gene expression was most robust for liver and kidney in which Ct values were between 20–25 for β-actin and 10–15 for S18 expression, respectively. Constitutive gene expression was generally the same among control and AFB1 groups except for kidney S18 which showed slight differences. However, RNA from FFPE lung samples demonstrated relatively weak expression with mean Ct values of about ≥30 for β-actin and S18. Thus, larger ranges in RNA size (liver and kidney > lung) corresponded to increased expression (lower Ct values) of two benchmark housekeeping genes. Conversely, we note the relationship between increased Ct values and smaller RNA size range (RNA degradation) in lung.

DISCUSSION

Retrospective evaluation of gene signatures using archived FFPE samples can be an important capability for toxicology. Testing the accuracy and specificity of gene signatures formulated by predictive models for carcinogenicity or screening for new or hypothesis-driven transcripts would be facilitated by the use of archival samples. In this study, we demonstrated that molecular analyses could be performed on RNA extracted and amplified from FFPE rat tissues preserved for four years. Critical features of the process included deparaffinization, protein digestion, silica-gel isolation, and DNase I digestion to isolate degraded but analytically useful RNA. Use of random hexamers for reverse transcriptase reactions and primers for relatively short amplicons were important steps in using degraded RNA as a template for amplification in qPCR.[7, 48] qPCR has been used to obtain gene expression data from FFPE samples from different tissue types and organs, often with tumor specimens to improve prognostic accuracy in clinical care.[7, 12, 15, 49] For example, RNA from FFPE samples of 153 breast cancer patients were used to develop an 8-gene qPCR gene expression score of prognostic value that could be reasonably implemented in clinical

settings without the need for fresh frozen RNA or more costly commercial signature arrays.[7] One recent study identified a 14 gene expression signature using qPCR with FFPE RNA from a 361 patient cohort to predict survival in nonsquamous, non-small-cell lung cancer.[50] Other investigations have also defined classifiers of disease progression or prognostic markers for invasive bladder cancer (eight genes)[51] or squamous cell carcinoma of lung (12 genes)[52] by qPCR analysis after gene selection from extensive microarray data sets, albeit from fresh-frozen materials. Importantly, the principle of qPCR-based screening of archival samples for focused sets of gene expression targets can similarly be exploited in toxicology studies.

Here, we tested a focused gene signature comprised of 14 transcripts and found agreement in direction and proportional change in transcript expression for Adam8, Mybl2, Akr7a3, Chd13, C8orf46 homolog, Ddit4l, Fhit, Abcc3, Abcb1b, Akr7a2 and Gst5a in FFPE samples compared to fresh frozen and microarray formats. Further studies will be needed to determine how the transcripts in this expression pattern might be of prognostic value for chemically-induced rat liver tumors. Ideally, a gene signature can be formulated whose combined expression pattern can accurately predict the occurrence of hepatocellular carcinoma in premalignant tissue in rodents. Such attempts are already underway by preclinical safety testing consortiums; one such study used data generated from more than 900 study-diverse liver samples in studies involving 66 various compound exposures to predict non-genotoxic heptocarcinogens from a 22-gene signature qPCR array platform.[53] Signature specificity and sensitivity for predicting nongenotoxic carcinogens were 67% and 59%, respectively, in which compounds were best classified with expression data from short-term repeat dose exposures. Among their findings was that modes of action for nongenotoxic and genotoxic compound could be discriminated based on the expression of specific genes.

The selection of transcripts for qPCR testing in our FFPE samples was based on informative genes from modeling of liver microarray data and genes responding to AFB1 exposure. These included probes representing nine upregulated (>3 fold), three moderately upregulated (2–3 fold) and two downregulated (<3 fold) transcripts. While eleven genes were concordant across platforms, three transcripts showed some variance, including Grin2c (upregulated), Wwox (moderately upregulated), and Cxlc1 (down regulated). Cxcl1 (GRO/Cinc-1) is a rat chemokine for neutrophils (similar to IL-8) that was reduced about 2 to 3 fold by microarray and qPCR, respectively, using RNA from fresh frozen tissue but it increased slightly above control in FFPE liver (1.2 fold). Since no significant differences in Cxcl1 were found among the three expression platforms, we would attribute these discrepancies to a minimal immune response in liver to AFB1 exposure. For Wwox, this transcript was generally lowered by hepatocarcinogen models[17] but showed a marginal increase of 1.3 fold in AFB1-treated rats by microarray analysis compared to a slightly decreased expression by qPCR of RNA from fresh frozen liver (1.6 fold decrease) and no change in FFPE liver (1.03 fold decrease) from the same animals. The reason for this discordance is not known but it may either reflect regional differences within the liver or that such small expression differences cannot be discriminated by qPCR. Finally, the transcript for the glutamate receptor subunit Grin2c was significantly increased by AFB1 in microarray analysis (18.1 fold increase) and by qPCR of RNA from FFPE sampling (4.5 fold increase) but could not be similarly reproduced using RNA from fresh frozen tissue (4.5 fold reduction) despite testing multiple qPCR primer sets across the length of the transcript including the 3′ portion. The length of the Grinc2c transcript is 4388 nt and the microarray probe was complementary to the 3′-end of the transcript. Our qPCR data indicated Grin2C was a relatively low expression transcript (Ct values of 27–32 for various primer sets). We used the same RNA extracted from fresh frozen tissue for qPCR that was used for microarray analysis, that was of high quality with intact 28S and 18S peaks and that showed concordance of all transcripts except Wwox and

Grin2c for these two platforms (Figure 1). We surmise that varying results for Grin2C might relate to differences in amplification efficiencies between microarray and qPCR procedures for this particularly long transcript of low copy number. Based on our limited gene set, retrospective testing of FFPE samples for generating gene signatures might include (where possible) moderately well expressed genes that are not inordinately large in length and at least a 2–3 fold expression difference from reference groups. We also recognize that amplification of low copy number transcripts can be particularly challenging with suboptimal RNA which can be addressed by using larger input amounts of RNA, mRNA isolation, use of gene-specific primers (instead of random hexamers) or nested primer sets. Use of gene signatures comprised of multiple transcripts chosen from the numerous critical biological pathways altered by chemical exposure can minimize reliance on single transcript biomarkers.[54] Furthermore, qPCR screening of archival training sets of multiple transcripts to remove technically or biologically variable transcripts is common practice in designing a robust gene signature prior to application in test samples.[50]

In our study, nucleic acid preservation took place under near optimal conditions in which 24hr formalin fixation was immediately followed by dehydration and paraffin embedding. The stability of the nucleic acids is dependent on fixation time in NBF and other variables such as pH, temperature, thickness of the tissues, type of tissues, tissue quality and isolation method, penetration of the fixation buffer into the tissue and efficiency of protein cross-linking.[1, 15, 48, 55] Among these factors, sample duration in formalin is likely of highest importance since increased tissue crosslinking occurs during prolonged fixation and reduces RNA yield and quality.[2] One study found that the yield of extractable RNA and DNA of human FFPE liver samples fixed in NBF from 2 weeks to 8 months was usable for qPCR but signal diminished with long fixation times as did RNA fragment size.[56] Once tissues are embedded in paraffin, nucleic acids and protein are relatively well maintained over time. However, RNA from archival FFPE breast cancer tissue isolated after six years was less degraded and of larger molecular weight than RNA isolated after seventeen years, suggesting that some nucleic acid fragmentation might still occur in paraffin blocks. Until such time that newer methods of tissue fixation without formaldehyde[57, 58] come into routine use for improved perservation of nucleic acids and cell structure for histology, the available data indicates that minimizing formalin-based fixation time before paraffin embedding is extremely useful for histopathology and downstream molecular analyses. Furthermore, the precise amount of time that tissues spend in fixative prior to parffin embedding is valuable metadata worth capturing for future archival studies.

After oral AFB1 exposure, gene expression changes were most evident in liver, the primary organ for AFB1 activation and conjugation. Even though kidney is a secondary target for AFB1 carcinogenesis[18], only Abcb1b was significantly increased in this organ. This observation suggests the xenosensor activity of Abcb1b was likely responding to AFB1 or its metabolites, but we speculate there was insufficient toxicity at this exposure (90 days, 1 ppm) to induce detoxication genes such as Akr7a3, Gst5a or other transcripts in the signature. In addition, it is possible that a microarray analysis of kidney might show expression changes in other transcripts not measured here, given availability of fresh frozen RNA.

In lung, we found relatively low and inconsistent gene expression from extracted FFPE lung RNA even though the RIN values were comparable among all three tissues. We considered whether genes in the signature were not expressed in rat lung and therefore not detectable. However, a query of a curated gene expression database (http://www.nextbio.com) suggested that each transcript could be detected under various treatment conditions (Supplemental Table 1), although we cannot completely discount that relatively lower copy numbers in lung compared to liver and kidney could make detection of some transcripts

more challenging. A more attractive explanation for the inconsistent qPCR data observed from lung was the comparatively poor RNA quality. The assessment of RNA quality by the RIN value takes into account the fractional area of 18S and 28S regions compared to total, as well as the heights of 28S (most degradation-sensitive) and 18S peaks and other factors in deriving a score that ranges from 1 to 10 (1 is the most degraded profile and 10 is the most intact).[59] RIN values of 2 for FFPE samples as found in our study indicate a loss of both 18S and 28S peaks and accumulation of low molecular weight RNA species.[59] However, we found the RIN value was not as discriminating for downstream analysis of FFPE RNA as the size range of RNA since liver and kidney contained RNA sizes of 2000–4000 nt which gave more consistent qPCR data than the smaller range of lung (≤500 nt). Freidin et al[60] described poor gene expression in FFPE lung samples compared to robust profiling from RNA of fresh or frozen lung samples. Others have found that prolonged NBF fixation (>24 hr) of lung tissue reduces RT-PCR success.[58] These reports and the less robust qPCR data from lung in our study suggest special care may be needed for archival preservation of this organ for later molecular analysis. Our observations suggest that expression of housekeeping genes like β-actin, S18 or others provide a functional readout of FFPE RNA integrity and, in combination with molecular sizing, are informative criteria to judge the usefulness of specific archival specimens.

One finding of interest was that amplification products up to 500 nt in length could be formed from cDNA of Akr7a3 and Ddit4l transcripts in FFPE RNA that could be cloned and sequenced. This capability could be of value in querying archival samples to detect specific mutations, synonomous substitutions as we report for Ddit4l, polymorphisms, splice variants, or other alterations in transcript expression. The target amplicon size for successful amplification in FFPE RNA samples is partly a function of FFPE RNA quality, median length of RNA fragments and relative cellular expression level of the specific transcript of interest. For example, the Akr7a3 is a well-expressed gene which could be cloned up to 499 nt (~500 nt) in our experiments although this band was not as intense as bands from amplicons 200 to 300 nt in length. The upper limit for amplification and cloning might exceed 500 nt for even more highly expressed transcripts and conversely might be somewhat less for lower expressed genes. Although we did not try additional measures to improve amplification of FFPE RNA, others have found that heating RNA at 70°C for 1 hr in Tris-EDTA buffer prior to RT-PCR removed almost all methylol groups which restored template integrity and PCR amplification to produce longer amplicons than without heating.[61] As previously mentioned, the general integrity, quality, extractability and fate of nucleic acids will decline with increasing time spent in formaldehyde solution. Inclusion of neutral buffer in 4% formalin solutions will slow but not stop the process of nucleic acid degradation. While the tissue processing steps prior to paraffin embedding are not without hazard to cellular structures and biomolecules, nucleic acids are better preserved in FFPE blocked tissues over time than in formalin solutions. However, there are many reasons aside from commitment of resources that not all preserved clinical and preclinical tissues are reduced to paraffin blocks. A less obvious but important reason is to maintain the structural integrity of the specimen for the flexibility of choosing the cut surface for histologic examination at some later time. Use of advanced, non-formaldehyde fixatives will provide even further flexibility to molecular toxicology in the future.

Summary

Gene expression studies in chemically-exposed rodents can elucidate key molecular events preceding toxicity phenotypes in controlled exposure environments with minimal genetic variation. Here, using qPCR, we evaluated a discrete signature derived from prior transcript analysis with genes representing cell cycle progression, response to DNA damage, xenosensor and detoxication systems, and successfully applied the signature to RNA

extracted from FFPE tissue compared with RNA extracted from corresponding fresh frozen tissues. This supports a conclusion that this signature and others can be evaluated in archival tissues from historical toxicology studies. Several new fixation protocols encouragingly show preservation of RNA, DNA, proteins and phosphoproteins in necropsied tissues[57, 58] but long-term storage has not yet been evaluated. The considerable resources expended on collecting and providing long-term storage of fresh frozen tissue for later molecular analysis make several innovative molecular platforms attractive for their compatibility with FFPE tissues to profile individual genes or to conduct genome-wide studies (Figure 8). We conclude that the ability to conduct retrospective evaluations of gene signatures in archival tissues is an important toxicological tool in reducing animal use by more fully interrogating prior studies and in determining critical molecular events as they relate to chemically-induced disease.

Supplementary Material

Refer to Web version on PubMed Central for supplementary material.

Acknowledgments

Funding Support: This research was supported by the Intramural Research Programs of the National Toxicology Program Division and Division of Intramural Research at the National Institute of Environmental Health Sciences of the NIH. The statements, opinions, or conclusions contained therein do not necessarily represent the statements, opinions, or conclusions of NIH or the United States government.

The authors would like to thank Drs. Arun Pandiri and Chad Blystone for critical review of the article. The technical assistance from the NIEHS Microarray Core of Laura Wharey for Bioanalyzer analysis, and advice in qPCR of Dr. Kevin Gerrish and Mr. Rick Fannin are appreciated.

Abbreviations

AFB1	Aflatoxin B1
Abcb1b	ATP-binding cassette, subfamily B (MDR/TAP), member 1B (P-glycoprotein/ multidrug resistance 1)
Abcc3	ATP-binding cassette, sub-family C (CFTR/MRP), member 3 (multidrug resistance associated protein)
Adam8	A disintegrin and metalloproteinase domain-containing, protein 8
Akr7a2	aldo-keto reductase family 7, member A2
Akr7a3	aldo-keto reductase family 7, member A3 (aflatoxin aldehyde reductase)
bDNA	branched DNA assay amplification for captured RNA
bp	base pair
c8orf46	chromosome 8 open reading frame 46 homolog
Cdh13	cadherin 13 (H-cadherin, heart)
CDS	(coding sequencing start site)
Cxcl1	chemokine (C-X-C motif) ligand 1
DASL	cDNA-mediated Annealing, Selection, Extension and Ligation analysis
Dditl	DNA-damage-inducible transcript 4-like
FF	fresh frozen

FFPE	formalin-fixed paraffin embedded
Fhit	fragile histidine triad gene
For	forward
Grin2c	Glutamate receptor, ionotropic, N-methyl D-aspartate 2C
ISH	in situ hybridization
Gst5a	glutathione S-transferase 5-α
HCC	hepatocellular carcinoma
MA	microarray
Mybl2	v-myb myeloblastosis viral oncogene homolog (avian)-like2
NBF	neutral buffered formalin
nt	nucleotide
qNPA	quantitative Nuclease, Protection Assay
qPCR	quantitative polymerase chain reaction
Rev	reverse
RIN	RNA integrity number
RT	reverse transcriptase
SVM	support vector machine
Wwox	WW domain containing oxidoreductase (fragile site FRA16D)
3′-Seq	NextGen sequencing for FFPE adapted toward 3′-region of transcripts

References

1. Klopfleisch R, Weiss AT, Gruber AD. Excavation of a buried treasure--DNA, mRNA, miRNA and protein analysis in formalin fixed, paraffin embedded tissues. Histol Histopathol. 2011; 26:797–810. [PubMed: 21472693]
2. Ludyga N, Grunwald B, Azimzadeh O, Englert S, Hofler H, Tapio S, Aubele M. Nucleic acids from long-term preserved FFPE tissues are suitable for downstream analyses. Virchows Arch. 2012
3. Ribeiro-Silva A, Zhang H, Jeffrey SS. RNA extraction from ten year old formalin-fixed paraffin-embedded breast cancer samples: a comparison of column purification and magnetic bead-based technologies. BMC Mol Biol. 2007; 8:118. [PubMed: 18154675]
4. Abdueva D, Wing M, Schaub B, Triche T, Davicioni E. Quantitative expression profiling in formalin-fixed paraffin-embedded samples by affymetrix microarrays. J Mol Diagn. 2010; 12:409–417. [PubMed: 20522636]
5. Linton K, Hey Y, Dibben S, Miller C, Freemont A, Radford J, Pepper S. Methods comparison for high-resolution transcriptional analysis of archival material on Affymetrix Plus 2.0 and Exon 1.0 microarrays. Biotechniques. 2009; 47:587–596. [PubMed: 19594443]
6. Scicchitano MS, Dalmas DA, Bertiaux MA, Anderson SM, Turner LR, Thomas RA, Mirable R, Boyce RW. Preliminary comparison of quantity, quality, and microarray performance of RNA extracted from formalin-fixed, paraffin-embedded, and unfixed frozen tissue samples. Journal of Histochemistry & Cytochemistry. 2006; 54:1229–1237. [PubMed: 16864893]
7. Sanchez-Navarro I, Gamez-Pozo A, Pinto A, Hardisson D, Madero R, Lopez R, San Jose B, Zamora P, Redondo A, Feliu J, Cejas P, Gonzalez Baron M, Angel Fresno Vara J, Espinosa E. An 8-gene qRT-PCR-based gene expression score that has prognostic value in early breast cancer. BMC Cancer. 2010; 10:336. [PubMed: 20584321]

8. Xie Y, Xiao G, Coombes KR, Behrens C, Solis LM, Raso G, Girard L, Erickson HS, Roth J, Heymach JV, Moran C, Danenberg K, Minna JD, Wistuba II. Robust gene expression signature from formalin-fixed paraffin-embedded samples predicts prognosis of non-small-cell lung cancer patients. Clin Cancer Res. 2011; 17:5705–5714. [PubMed: 21742808]
9. Hall JS, Leong HS, Armenoult LS, Newton GE, Valentine HR, Irlam JJ, Moller-Levet C, Sikand KA, Pepper SD, Miller CJ, West CM. Exon-array profiling unlocks clinically and biologically relevant gene signatures from formalin-fixed paraffin-embedded tumour samples. Br J Cancer. 2011; 104:971–981. [PubMed: 21407225]
10. Saleh A, Zain RB, Hussaini H, Ng F, Tanavde V, Hamid S, Chow AT, Lim GS, Abraham MT, Teo SH, Cheong SC. Transcriptional profiling of oral squamous cell carcinoma using formalin-fixed paraffin-embedded samples. Oral Oncol. 2010; 46:379–386. [PubMed: 20371203]
11. Kennedy RD, Bylesjo M, Kerr P, Davison T, Black JM, Kay EW, Holt RJ, Proutski V, Ahdesmaki M, Farztdinov V, Goffard N, Hey P, McDyer F, Mulligan K, Mussen J, O'Brien E, Oliver G, Walker SM, Mulligan JM, Wilson C, Winter A, O'Donoghue D, Mulcahy H, O'Sullivan J, Sheahan K, Hyland J, Dhir R, Bathe OF, Winqvist O, Manne U, Shanmugam C, Ramaswamy S, Leon EJ, Smith WI Jr, McDermott U, Wilson RH, Longley D, Marshall J, Cummins R, Sargent DJ, Johnston PG, Harkin DP. Development and independent validation of a prognostic assay for stage II colon cancer using formalin-fixed paraffin-embedded tissue. J Clin Oncol. 2011; 29:4620–4626. [PubMed: 22067406]
12. Jacobson TA, Lundahl J, Mellstedt H, Moshfegh A. Gene expression analysis using long-term preserved formalin-fixed and paraffin-embedded tissue of non-small cell lung cancer. Int J Oncol. 2011; 38:1075–1081. [PubMed: 21305253]
13. Yeatts K. Quantitative polymerase chain reaction using the comparative C q method. Methods Mol Biol. 2011; 700:171–184. [PubMed: 21204034]
14. Casado E, Garcia VM, Sanchez JJ, Blanco M, Maurel J, Feliu J, Fernandez-Martos C, de Castro J, Castelo B, Belda-Iniesta C, Sereno M, Sanchez-Llamas B, Burgos E, Garcia- Cabezas MA, Mancenido N, Miquel R, Garcia-Olmo D, Gonzalez-Baron M, Cejas P. A combined strategy of SAGE and quantitative PCR Provides a 13-gene signature that predicts preoperative chemoradiotherapy response and outcome in rectal cancer. Clin Cancer Res. 2011; 17:4145–4154. [PubMed: 21467161]
15. Roberts L, Bowers J, Sensinger K, Lisowski A, Getts R, Anderson MG. Identification of methods for use of formalin-fixed, paraffin-embedded tissue samples in RNA expression profiling. Genomics. 2009; 94:341–348. [PubMed: 19660539]
16. Booker SM. NTP archives: the ex-files. Environ Health Perspect. 1997; 105:1182–1184. [PubMed: 9432466]
17. Auerbach SS, Shah RR, Mav D, Smith CS, Walker NJ, Vallant MK, Boorman GA, Irwin RD. Predicting the hepatocarcinogenic potential of alkenylbenzene flavoring agents using toxicogenomics and machine learning. Toxicol Appl Pharmacol. 2010; 243:300–314. [PubMed: 20004213]
18. Butler WH, Greenblatt M, Lijinsky W. Carcinogenesis in rats by aflatoxins B1, G1, and B2. Cancer Res. 1969; 29:2206–2211. [PubMed: 4318833]
19. Wogan GN, Kensler TW, Groopman JD. Present and future directions of translational research on aflatoxin and hepatocellular carcinoma. A review. Food Addit Contam Part A Chem Anal Control Expo Risk Assess. 2011:1–9.
20. Wogan GN, Newberne PM. Dose-response characteristics of aflatoxin B1 carcinogenesis in the rat. Cancer Res. 1967; 27:2370–2376. [PubMed: 4295478]
21. Calvisi DF, Simile MM, Ladu S, Frau M, Evert M, Tomasi ML, Demartis MI, Daino L, Seddaiu MA, Brozzetti S, Feo F, Pascale RM. Activation of v-Myb avian myeloblastosis viral oncogene homolog-like2 (MYBL2)-LIN9 complex contributes to human hepatocarcinogenesis and identifies a subset of hepatocellular carcinoma with mutant p53. Hepatology. 2011; 53:1226–1236. [PubMed: 21480327]
22. Hernandez I, Moreno JL, Zandueta C, Montuenga L, Lecanda F. Novel alternatively spliced ADAM8 isoforms contribute to the aggressive bone metastatic phenotype of lung cancer. Oncogene. 2010; 29:3758–3769. [PubMed: 20453887]

23. Walsh N, Larkin A, Kennedy S, Connolly L, Ballot J, Ooi W, Gullo G, Crown J, Clynes M, O'Driscoll L. Expression of multidrug resistance markers ABCB1 (MDR-1/P-gp) and ABCC1 (MRP-1) in renal cell carcinoma. BMC urology. 2009; 9:6. [PubMed: 19552816]
24. Stathopoulos GP, Armakolas A. Differences in gene expression between individuals with multiple primary and single primary malignancies. International journal of molecular medicine. 2009; 24:613–622. [PubMed: 19787195]
25. Ellinger-Ziegelbauer H, Gmuender H, Bandenburg A, Ahr HJ. Prediction of a carcinogenic potential of rat hepatocarcinogens using toxicogenomics analysis of short-term in vivo studies. Mutat Res. 2008; 637:23–39. [PubMed: 17689568]
26. Iida M, Anna CH, Holliday WM, Collins JB, Cunningham ML, Sills RC, Devereux TR. Unique patterns of gene expression changes in liver after treatment of mice for 2 weeks with different known carcinogens and non-carcinogens. Carcinogenesis. 2005; 26:689–699. [PubMed: 15618236]
27. Nakayama K, Kawano Y, Kawakami Y, Moriwaki N, Sekijima M, Otsuka M, Yakabe Y, Miyaura H, Saito K, Sumida K, Shirai T. Differences in gene expression profiles in the liver between carcinogenic and non-carcinogenic isomers of compounds given to rats in a 28-day repeat-dose toxicity study. Toxicol Appl Pharmacol. 2006; 217:299–307. [PubMed: 17070881]
28. Kensler TW, Roebuck BD, Wogan GN, Groopman JD. Aflatoxin: a 50- year odyssey of mechanistic and translational toxicology. Toxicol Sci. 2011; 120(Suppl 1):S28–48. [PubMed: 20881231]
29. RoC. Aflatoxins. Rep Carcinog. 2011:32–34. [PubMed: 21829243]
30. Guengerich FP, Johnson WW, Shimada T, Ueng YF, Yamazaki H, Langouet S. Activation and detoxication of aflatoxin B1. Mutat Res. 1998; 402:121–128. [PubMed: 9675258]
31. Martinez I, Dimaio D. B-Myb, Cancer, Senescence, and MicroRNAs. Cancer Res. 2011; 71:5370–5373. [PubMed: 21828240]
32. Sala A, Casella I, Bellon T, Calabretta B, Watson RJ, Peschle C. B-myb promotes S phase and is a downstream target of the negative regulator p107 in human cells. J Biol Chem. 1996; 271:9363–9367. [PubMed: 8621601]
33. Guaiquil VH, Swendeman S, Zhou W, Guaiquil P, Weskamp G, Bartsch JW, Blobel CP. ADAM8 is a negative regulator of retinal neovascularization and of the growth of heterotopically injected tumor cells in mice. J Mol Med (Berl). 2010; 88:497–505. [PubMed: 20119708]
34. Cascorbi I. P-glycoprotein: tissue distribution, substrates, and functional consequences of genetic variations. Handb Exp Pharmacol. 2011:261–283. [PubMed: 21103972]
35. Knight LP, Primiano T, Groopman JD, Kensler TW, Sutter TR. cDNA cloning, expression and activity of a second human aflatoxin B1-metabolizing member of the aldo-keto reductase superfamily, AKR7A3. Carcinogenesis. 1999; 20:1215–1223. [PubMed: 10383892]
36. Ellis EM. Protection against aflatoxin B1 in rat--a new look at the link between toxicity, carcinogenicity, and metabolism. Toxicol Sci. 2009; 109:1–3. [PubMed: 19293422]
37. Nies AT, Konig J, Pfannschmidt M, Klar E, Hofmann WJ, Keppler D. Expression of the multidrug resistance proteins MRP2 and MRP3 in human hepatocellular carcinoma. Int J Cancer. 2001; 94:492–499. [PubMed: 11745434]
38. Nemoto K, Tanaka T, Ikeda A, Ito S, Mizukami M, Hikida T, Gamou T, Habano W, Ozawa S, Inoue K, Yoshida M, Nishikawa A, Degawa M. Super-induced gene expression of the N-methyl-D-aspartate receptor 2C subunit in chemical-induced hypertrophic liver in rats. J Toxicol Sci. 2011; 36:507–514. [PubMed: 22008526]
39. Andreeva AV, Kutuzov MA. Cadherin 13 in cancer. Genes Chromosomes Cancer. 2010; 49:775–790. [PubMed: 20607704]
40. Riou P, Saffroy R, Chenailler C, Franc B, Gentile C, Rubinstein E, Resink T, Debuire B, Piatier-Tonneau D, Lemoine A. Expression of T-cadherin in tumor cells influences invasive potential of human hepatocellular carcinoma. Faseb J. 2006; 20:2291–2301. [PubMed: 17077306]
41. Ueda S, Basaki Y, Yoshie M, Ogawa K, Sakisaka S, Kuwano M, Ono M. PTEN/Akt signaling through epidermal growth factor receptor is prerequisite for angiogenesis by hepatocellular carcinoma cells that is susceptible to inhibition by gefitinib. Cancer Res. 2006; 66:5346–5353. [PubMed: 16707461]

42. Corradetti MN, Inoki K, Guan KL. The stress-inducted proteins RTP801 and RTP801L are negative regulators of the mammalian target of rapamycin pathway. J Biol Chem. 2005; 280:9769–9772. [PubMed: 15632201]
43. Wang HW, Wu YH, Hsieh JY, Liang ML, Chao ME, Liu DJ, Hsu MT, Wong TT. Pediatric primary central nervous system germ cell tumors of different prognosis groups show characteristic miRNome traits and chromosome copy number variations. BMC Genomics. 2010; 11:132. [PubMed: 20178649]
44. Hayes JD, Pulford DJ, Ellis EM, McLeod R, James RF, Seidegard J, Mosialou E, Jernstrom B, Neal GE. Regulation of rat glutathione S-transferase A5 by cancer chemopreventive agents: mechanisms of inducible resistance to aflatoxin B1. Chem Biol Interact. 1998; 111–112:51–67.
45. Praml C, Schulz W, Claas A, Mollenhauer J, Poustka A, Ackermann R, Schwab M, Henrich KO. Genetic variation of Aflatoxin B1 aldehyde reductase genes (AFAR) in human tumour cells. Cancer Lett. 2008; 272:160–166. [PubMed: 18752886]
46. Hinshelwood A, McGarvie G, Ellis E. Characterisation of a novel mouse liver aldo-keto reductase AKR7A5. FEBS Lett. 2002; 523:213–218. [PubMed: 12123834]
47. McCurley AT, Callard GV. Characterization of housekeeping genes in zebrafish: male-female differences and effects of tissue type, developmental stage and chemical treatment. BMC Mol Biol. 2008; 9:102. [PubMed: 19014500]
48. Oberli A, Popovici V, Delorenzi M, Baltzer A, Antonov J, Matthey S, Aebi S, Altermatt HJ, Jaggi R. Expression profiling with RNA from formalin-fixed, paraffin-embedded material. BMC Med Genomics. 2008; 1:9. [PubMed: 18423048]
49. Sanchez-Navarro I, Gamez-Pozo A, Gonzalez-Baron M, Pinto-Marin A, Hardisson D, Lopez R, Madero R, Cejas P, Mendiola M, Espinosa E, Vara JA. Comparison of gene expression profiling by reverse transcription quantitative PCR between fresh frozen and formalin-fixed, paraffin-embedded breast cancer tissues. Biotechniques. 2010; 48:389–397. [PubMed: 20569212]
50. Kratz JR, He J, Van Den Eeden SK, Zhu ZH, Gao W, Pham PT, Mulvihill MS, Ziaei F, Zhang H, Su B, Zhi X, Quesenberry CP, Habel LA, Deng Q, Wang Z, Zhou J, Li H, Huang MC, Yeh CC, Segal MR, Ray MR, Jones KD, Raz DJ, Xu Z, Jahan TM, Berryman D, He B, Mann MJ, Jablons DM. A practical molecular assay to predict survival in resected non-squamous, non-small-cell lung cancer: development and international validation studies. Lancet. 2012
51. Kim WJ, Kim EJ, Kim SK, Kim YJ, Ha YS, Jeong P, Kim MJ, Yun SJ, Lee KM, Moon SK, Lee SC, Cha EJ, Bae SC. Predictive value of progressionrelated gene classifier in primary non-muscle invasive bladder cancer. Mol Cancer. 2010; 9:3. [PubMed: 20059769]
52. Zhu CQ, Strumpf D, Li CY, Li Q, Liu N, Der S, Shepherd FA, Tsao MS, Jurisica I. Prognostic gene expression signature for squamous cell carcinoma of lung. Clin Cancer Res. 2010; 16:5038–5047. [PubMed: 20739434]
53. Fielden MR, Adai A, Dunn RT 2nd, Olaharski A, Searfoss G, Sina J, Aubrecht J, Boitier E, Nioi P, Auerbach S, Jacobson-Kram D, Raghavan N, Yang Y, Kincaid A, Sherlock J, Chen SJ, Car B. Development and evaluation of a genomic signature for the prediction and mechanistic assessment of nongenotoxic hepatocarcinogens in the rat. Toxicol Sci. 2011; 124:54–74. [PubMed: 21813463]
54. Chang C, Wang J, Zhao C, Fostel J, Tong W, Bushel PR, Deng Y, Pusztai L, Symmans WF, Shi T. Maximizing biomarker discovery by minimizing gene signatures. BMC Genomics. 2011; 12(Suppl 5):S6. [PubMed: 22369133]
55. Kiernan JA. Formaldehyde, formalin, paraformaldehyde and glutaraldehyde: what they are and what they do. Microscopy Today, 00-1. 2000:8–12.
56. Ferruelo A, El-Assar M, Lorente JA, Nin N, Penuelas O, Fernandez-Segoviano P, Gonzalez C, Esteban A. Transcriptional profiling and genotyping of degraded nucleic acids from autopsy tissue samples after prolonged formalin fixation times. Int J Clin Exp Pathol. 2011; 4:156–161. [PubMed: 21326810]
57. Mueller C, Edmiston KH, Carpenter C, Gaffney E, Ryan C, Ward R, White S, Memeo L, Colarossi C, Petricoin EF 3rd, Liotta LA, Espina V. One-step preservation of phosphoproteins and tissue morphology at room temperature for diagnostic and research specimens. PLoS One. 2011; 6:e23780. [PubMed: 21858221]

58. Turashvili G, Yang W, McKinney S, Kalloger S, Gale N, Ng Y, Chow K, Bell L, Lorette J, Carrier M, Luk M, Aparicio S, Huntsman D, Yip S. Nucleic acid quantity and quality from paraffin blocks: Defining optimal fixation, processing and DNA/RNA extraction techniques. Exp Mol Pathol. 2011; 92:33–43. [PubMed: 21963600]

59. Schroeder A, Mueller O, Stocker S, Salowsky R, Leiber M, Gassmann M, Lightfoot S, Menzel W, Granzow M, Ragg T. The RIN: an RNA integrity number for assigning integrity values to RNA measurements. BMC Mol Biol. 2006; 7:3. [PubMed: 16448564]

60. Freidin MB, Bhudia N, Lim E, Nicholson AG, Cookson WO, Moffatt MF. Impact of collection and storage of lung tumor tissue on whole genome expression profiling. J Mol Diagn. 2012; 14:140–148. [PubMed: 22240448]

61. Masuda N, Ohnishi T, Kawamoto S, Monden M, Okubo K. Analysis of chemical modification of RNA from formalin-fixed samples and optimization of molecular biology applications for such samples. Nucleic Acids Res. 1999; 27:4436–4443. [PubMed: 10536153]

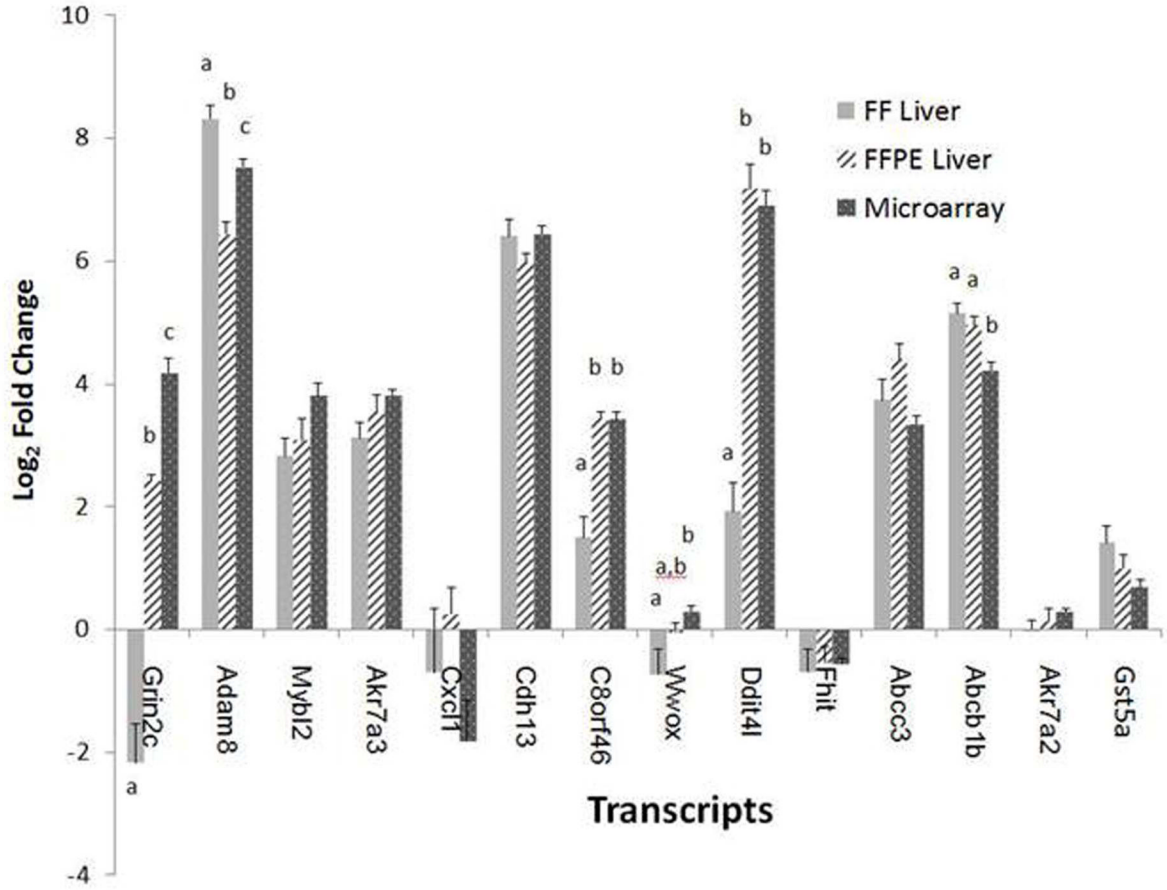

Figure 1. qPCR of AFB1 gene signature

Bar graph shows fold changes of aflatoxin B1 (AFB1)-induced gene expression in rat liver samples comparing qPCR data of formalin-fixed paraffin embedded (FFPE) liver RNA and fresh frozen (FF) liver RNA and microarray (MA) data published in Auerbach et al.[17] Male F344 rats were exposed subchronically to AFB1 in feed at 1 ppm as described in Methods. DNA microarray analysis was performed with Agilent 4x44K rat whole genome oligonucleotide arrays.[17] Based on microarray data, genes were selected for qPCR testing with FF liver and for comparative analysis with FFPE tissue blocks. Using the same animals from the microarray study, qPCR was performed with RNA extracted from either FF or FFPE samples. Bars represent means ± standard error of the mean (S.E.M.) at n=6 per group, which were compared by ANOVA and Tukey HSD post-hoc tests. For each gene, letters not shared among bars were different at $p \leq 0.05$.

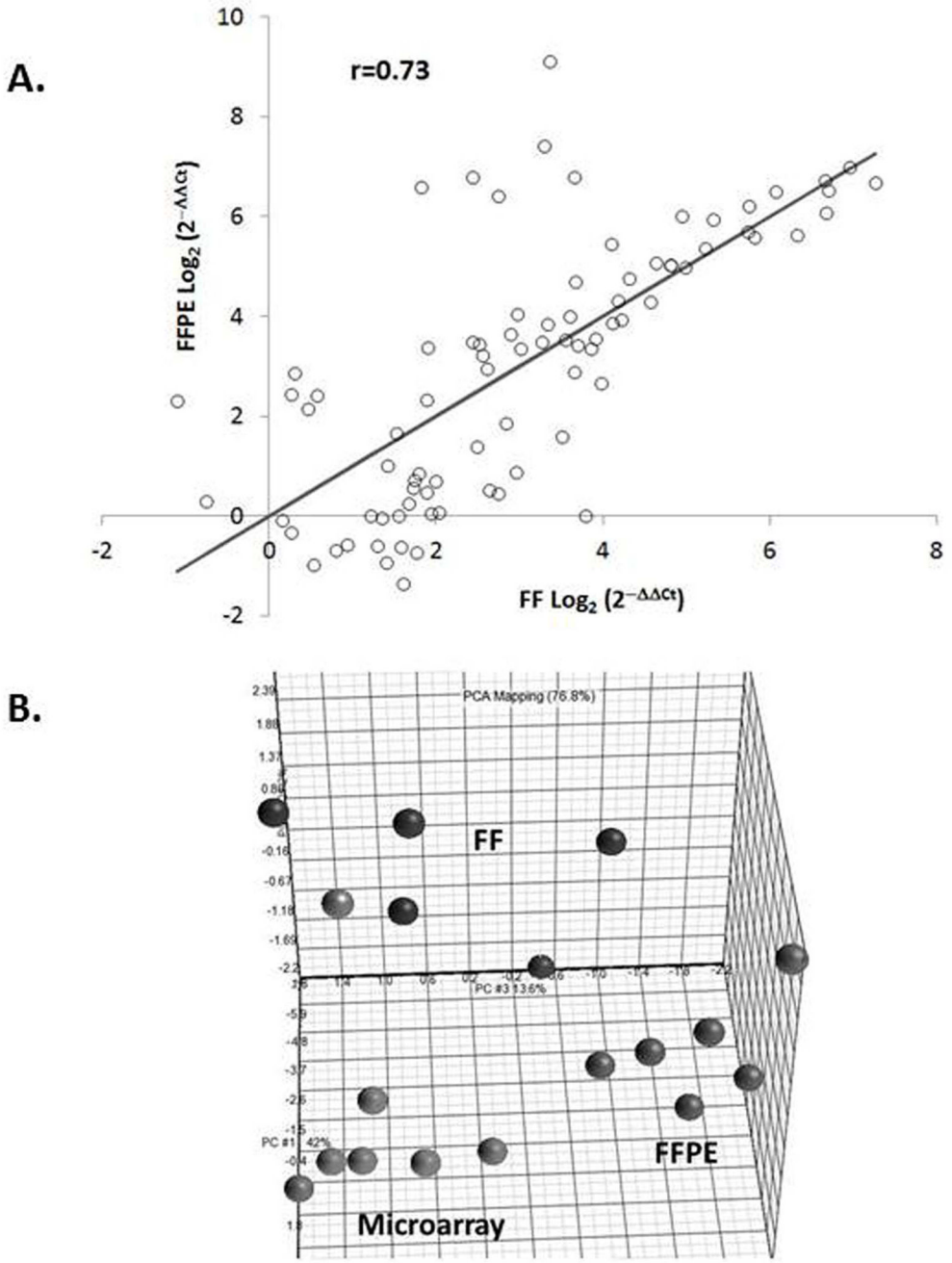

Figure 2. Regression analysis and principal component analysis (PCA) plots of liver gene expression data

Panel A. Regression analysis of AFB1-induced gene expression fold changes of transcripts analyzed by qPCR from fresh frozen (FF) or formalin-fixed paraffin embedded (FFPE) rat liver. Regression analysis was performed on fold changes for $2^{-\Delta\Delta Ct}$ data for qPCR analysis of 14 genes from fresh frozen and FFPE liver samples at n=6 per group. A significant positive correlation at $p \leq 0.05$ was determined for which an r^2 value of 0.73 was obtained. Panel B. PCA shows the relationships among AFB1-induced liver transcript changes for each animal among microarray, FF and FFPE platforms. The plot accounts for 77.5% of variability in the data.

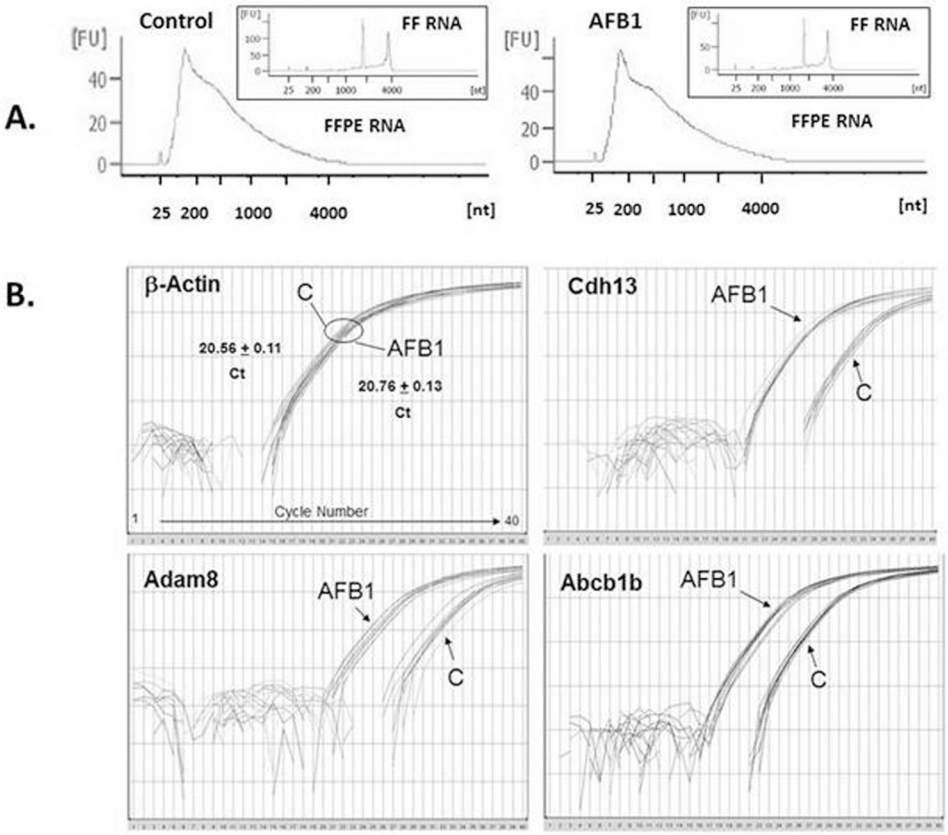

Figure 3. Molecular sizing of liver RNA and qPCR of AFB1-sensitive genes

Panel A shows representative microfluidic separations of RNA (900 ng/μl) isolated from formalin fixed, paraffin embedded (FFPE) liver of a control (C) or aflatoxin (AFB1) exposed rat while the insets are separations of fresh frozen (FF) liver RNA from the identical, respective animal. [FU] are fluorescent units; [nt] are number of nucleotides. Panel B shows overlays of amplification plots of cycle number vs fluorescence (ΔRn) for β-actin, Cdh13, Adam8 and Abcb1b transcripts for samples from control and AFB1 treatments. Each curve is a representative qPCR reaction from an individual control or AFB1 treated animal at n=6/group. Ct values for β-actin (mean ± SEM) were not significantly different between treatments so that their values were used for normalization of other transcripts. Relative fold changes from control were calculated by the $2^{-\Delta\Delta Ct}$ method normalized against β-actin expression for each transcript as summarized in Figure 1.

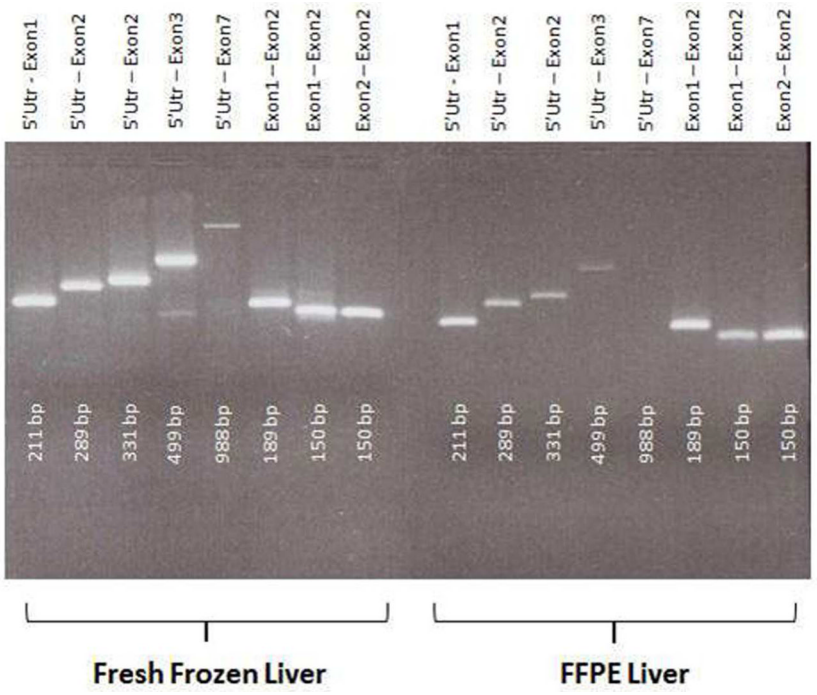

Figure 4. Exon amplification of Akr7a3 transcript from cDNA of Fresh Frozen (FF) and Formalin Fixed Paraffin Embedded (FFPE) liver

Amplicons were from the 5′-untranslated region (5′-Utr) to Exons 1, 2, 3 and 7, and from Exon 1–2 or Exon 2 only. Results are representative of an experiment using fresh frozen and FFPE RNA from the same animal (AFB1). Three animals were evaluated and showed similar results. Note the uniform staining intensity of amplicons in fresh frozen liver while amplicons from paraffin samples (FFPE) liver were of decreased intensity with increasing product length, becoming faint at 499 bp and undetectable for the longest amplicon at 988 bp. Each PCR reaction was conducted for 35 cycles using primers with similar Tm values.

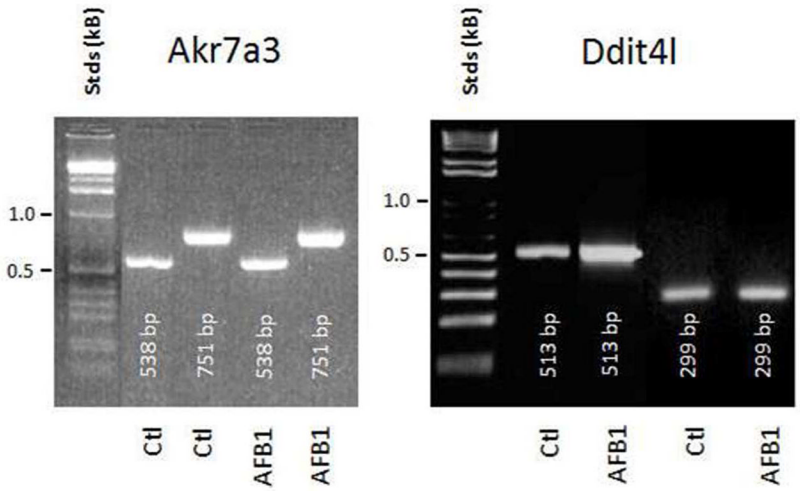

Figure 5. PCR cloning of coding regions for two AFB1-responsive genes

PCR primers were designed to form products that encompassed the coding region for each gene. Products were detected by UV light after separation on 2% agarose-ethidium bromide gels. For Akr7a3, the left panel shows 538 bp and 751 bp amplicons while the right panel contains Ddit4l amplicons of 296 bp and 513 bp sizes. cDNA was extracted from each band, cloned and Sanger sequenced. The identity of each band was confirmed by comparison to the mRNA sequence for Akr7a3 (NM_013215) and Ddit4l (NM_080399). Representative PCR reactions at 35 cycles are shown for control and AFB1 samples from fresh frozen liver.

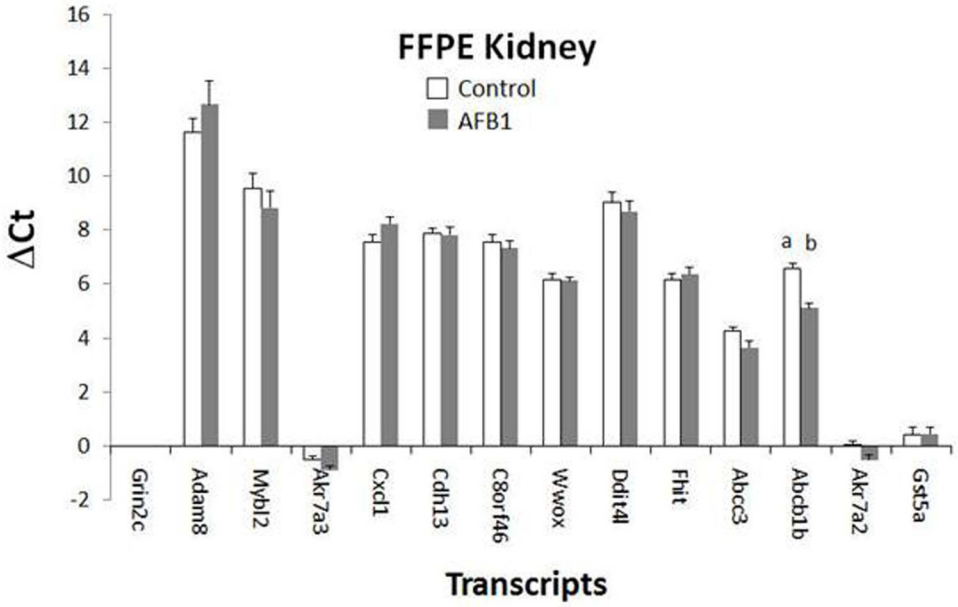

Figure 6. qPCR of RNA isolated from kidney in paraffin blocks

Rats were exposed to AFB1 in feed for 90 days as described in Figure 1. Kidneys were formalin fixed, embedded in paraffin (FFPE), and after use, blocks were placed in archival storage. Subsequently, qPCR was performed after extraction of RNA from kidney in paraffin blocks. Data were normalized as the difference of Ct values for each gene and β-actin (ΔCt). Bars represent means ± standard error of the mean (S.E.M) at n=6 per group which were analyzed by ANOVA followed by comparison of control and AFB1 treatments using the Tukey HSD post-hoc test. For each gene, letters not shared among bars were different at $p \leq 0.05$.

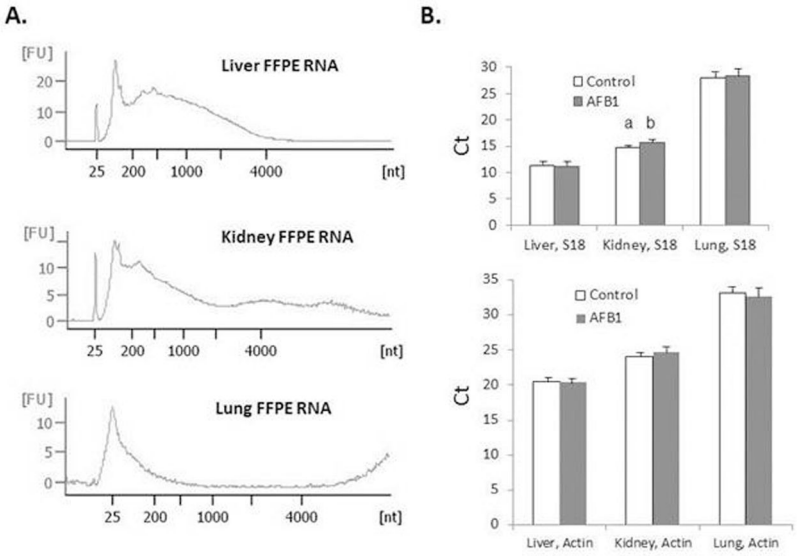

Figure 7. Molecular sizing and qPCR of liver, kidney and lung RNA

In Panel A, microcapillary separation of RNA was conducted to show the distribution of molecular weight sizes present in representative samples of liver, kidney and lung at 250 ng/μl. Fluorescent units [FU] and the number of nucleotides [nt] are on the 'y' and 'x' axis, respectively. Note flattening of fluorescence curve for high molecular sizes >4000 region in liver, while kidney and lung still show some fluorescence in this region (not RNA). In addition, note changes in shape of fluorescence-sizing curve of liver FFPE RNA in Figures 3a and 7a due to input differences in RNA concentration. Panel B presents qPCR data of constitutive genes, β-actin and S18, after RNA isolation from liver, kidney and lung in paraffin blocks. Bars represent means ± standard error of the mean (S.E.M) at n=6 per group which were analyzed by ANOVA and compared by Tukey HSD post-hoc tests. For each gene, letters not shared among bars were different at $p \leq 0.05$.

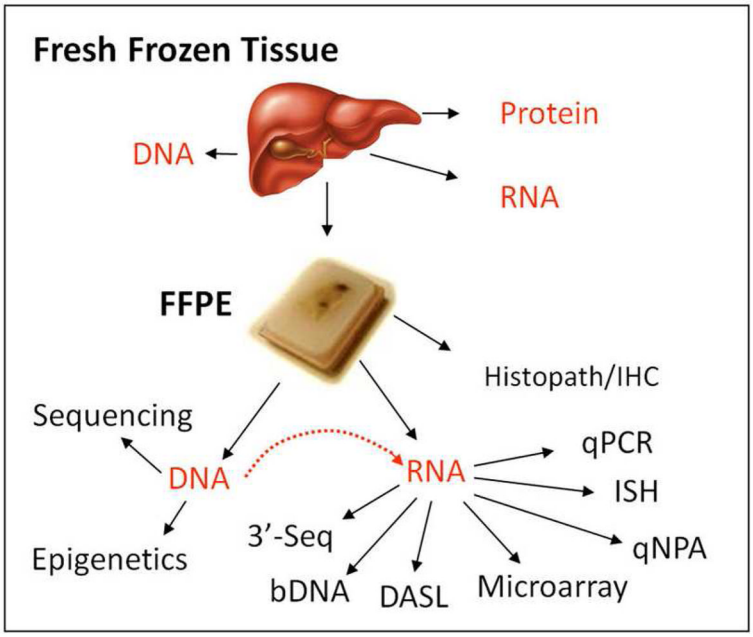

Figure 8. Expression platforms for archival specimens

Gene expression based on protein, RNA and DNA analysis in fresh frozen tissues is often preferred for the greatest flexibility in biochemical and molecular analysis to complement conventional histopathology and immunohistochemistry (Histopath/IHC). However, several molecular platforms are compatible with formalin fixed paraffin embedded (FFPE) tissues for analysis of individual genes or genomic level studies. Platforms for FFPE RNA include qPCR (quantitative or real-time PCR), ISH (In Situ Hybridization) and qNPA (quantitative Nuclease Protection Assay), which can measure transcripts in single or multiplexed modes. Sub-genomic analysis can be conducted with oligonucleotide-based microarrays such as DASL (cDNA-mediated annealing, selection, extension, and ligation analysis) and bDNA (branched-chain DNA amplification for captured RNA) or genome-wide analysis by 3′-Seq (NextGen sequencing for FFPE adapted toward 3′-region of transcripts) or hybridization-based microarrays. Further, paraffin samples can be extracted for genomic or methylated DNA and be analyzed by sequencing or specialized microarray formats to link epigenetic effects (dotted arrow) with RNA expression.

Table 1

Gene Signature of AFB1 Toxicity[a]

Probe Name	Gene Symbol	Function
A_44_P869415	Wwox	Fragile site gene, role in cancer
A_44_P331276	Fhit	Fragile site gene, role in cancer
A_44_P866659	Adam8	Disintegrin/metalloprotease, Egf domains
A_44_P884766	C8orf46	Unknown, genotoxic responsive
A_44_P653701	Mybl2	B-Myb (myeloblastosis oncogene homolog)
A_44_P141897	Abc1b1	Mdr1 drug transporter
A_44_P561084	Cdh13	Cell growth, methylated in many cancers
A_42_P738337	Grin2c	NMDA glutamate receptor, ion channel
A_42_P841193	Ddit4l	DNA-damage inducible transcript 4-like
A_44_P221974	Abcc3	Bile acid transporter
A_43_P11754	Akr7a3	Aldehyde reductase, AFB1-inducible
A_42_P473398	Cxcl1	Chemokine, cell growth
A_42_P624333	Akr7a2	Aldehyde reductase, AFB1-inducible
A_44_P492831	Gsta5	GST-S-transferase, AFB1-inducible

[a]Fourteen genes were chosen from a genome-wide hepatic gene expression study using Agilent 4X44K rat microarrays conducted on F344 male rats. Animals were exposed to a collection of structurally diverse liver carcinogens and non-carcinogens for 2, 14 or 90 days as described.[17] The top six probes in this table were among the most highly up- and down-regulated probes that were informative to multiple optimal hepatocarcinogen prediction models, while the following six probes were significantly responsive to 90-day hepatocarcinogen treatment compared to non-carcinogens at 90 days. The last two probes were included as AFB1-responsive from this study and other studies. See Methods for further details.

Table 2

Primers for qPCR[a]

Gene	For/Rev	Sequence	NCBI RefSeq	Amplicon Size
Cxcl1	For	CAG ACA GTG GCA GGG ATT	NM_030845	91 bp
	Rev	TGG CTA TGA CTT CGG TTT G		
C8orf46	For	AGA GTA CCC AGC CCT TCC	NM_001109260	94 bp
	Rev	CCA CAT TTT TCG CAG GAT		
Ddit4l	For	TGC ACG TGA ACT TGG AAA	NM_080399	91 bp
	Rev	AGC GTG AGC TCA AAG GTC		
Grin2c	For	TGC ATC GAC ATC CTC AAA	NM_012575	99 bp
	Rev	CAC ACC ACG AAC CCT CTT		
Abcc3	For	TGC ACC AGA TGA AAA CCA	NM_080581	95 bp
	Rev	CTG TGT GGG TGC TGA GTG		
Cdh13	For	AAC CCA CAG ACC AAC GAG	NM_138889	82 bp
	Rev	TGA TCA GCA GGG TGT GAA		
Fhit	For	GAT GGT CCT GAA GCT GGA	NM_021774	77 bp
	Rev	CTG CGG AAG TCT CCT GAC		
Wwox	For	AGA GAT ACG ACG GGA GCA	NM_001106188	75 bp
	Rev	TAA CCA GGA CCA CCT TGC		
Abcb1b	For	CTC GGG AGC AGA AGT TTG	NM_012623	96 bp
	Rev	CGA AGG TGA TCC CAA AGA		
Mybl2	For	AGA ATG TCC AGC CTG TGG	NM_001106536	84 bp
	Rev	TGC TCT CCT CCT CCT TCA		
Adam8	For	GCT GGG CTC AAG CTA CAC	XM_001056204	116 bp
	Rev	GAG CCC TCA TAC CCT TCC		
Akr7a3	For	GAG CAG AAC TTG GCC TTG	NM_013215	75 bp
	Rev	GTT CCA GGC TTG GTC AAA		
Akr7a2	For	GAG CTT GGC TTG TCC AAC	NM_134407	74 bp
	Rev	ATC CAG CCG TTG CTT TTA		
Gsta5	For	GTG CAG ACC AAA GCC ATT	NM_001009920	79 bp
	Rev	TGA GGG CTC TCT CCT TCA		
Actb	For	AGG GTG TGA TGG TGG GTA	NM_031144	142 bp
	Rev	TGG TGC CAA ATC TTC TCC		
Rps18	For	CCT GCG GCT TAA TTT GAC	NM_213557	92 bp
	Rev	CCA CGG AAT CGA GAA AGA		

[a]For, Forward primer; Rev, Reverse Primer; NCBI RefSeq, reference sequence; RGD1561849 is the rat homolog to hu_C8orf46; Actb is β-actin; Rps18 is S18.